

required to explain fully the persistence of the disease in a metapopulation where there is no influx from an external source (5).

In summary, inclusion of a more realistic infection period in childhood disease models generates the high-frequency pulsing seen in the real data and produces more realistic levels of persistence, as reflected in the lower CCS. This improved fit is likely to be a generic result for infections that occur as self-extinguishing epidemics. More generally, this well-documented example underlines (25) the idea that the assumption of constant transition rates (and therefore exponentially distributed times), which is often made in ecology, may need to be reevaluated if we are to fully understand patterns of stochastic fluctuations and extinctions.

REFERENCES AND NOTES

1. M. S. Bartlett, *J. R. Stat. Soc. Ser. A* **120**, 48 (1957); B. M. Bolker and B. T. Grenfell, *Proc. R. Soc. London Ser. B* **251**, 75 (1993).
2. M. S. Bartlett, *J. R. Stat. Soc. Ser. A* **123**, 37 (1960).
3. F. L. Black, *J. Theor. Biol.* **11**, 207 (1966); A. P. Cliff, P. Haggett, J. K. Ord, G. R. Versey, *Spatial Diffusion: An Historical Geography of Epidemics in an Island Community* (Cambridge Univ. Press, Cambridge, 1981).
4. B. T. Grenfell, *J. R. Stat. Soc. Ser. B* **54**, 383 (1992).
5. ———, B. M. Bolker, A. Kleczkowski, *Proc. R. Soc. London Ser. B* **259**, 97 (1995).
6. R. M. Anderson and R. M. May, *Infectious Diseases of Humans* (Oxford Univ. Press, Oxford, 1992).
7. H. E. Soper, *J. R. Stat. Soc. Ser. A* **92**, 34 (1929).
8. P. E. M. Fine and J. A. Clarkson, *Int. J. Epidemiol.* **11**, 5 (1982); J. L. Aron and I. B. Schwartz, *J. Theor. Biol.* **110**, 665 (1984).
9. L. F. Olsen and W. M. Schaffer, *Science* **249**, 499 (1990).
10. D. Schenzle, *IMA J. Math. Appl. Med. Biol.* **1**, 169 (1984).
11. B. T. Grenfell, A. Kleczkowski, S. P. Ellner, B. M. Bolker, *Philos. Trans. R. Soc. London Ser. A* **348**, 515 (1994).
12. B. T. Grenfell, A. Kleczkowski, C. A. Gilligan, B. M. Bolker, *Stat. Methods Med. Res.* **4**, 160 (1995).
13. B. M. Bolker, *IMA J. Math. Appl. Med. Biol.* **10**, 83 (1993).
14. The standard RAS formulation categorizes individuals into four distinct age groups: under 6 (preschool), 6 to 10 (primary school), 10 to 20 (adolescents), and over 20 (adults). Within each class, the population is further subdivided into susceptible (S), exposed (E), infectious (I), and recovered (R) groups. There is a constant birth rate into the youngest age group, but movement between the other age classes occurs annually at the start of the school year. The transmission between and within each age class occurs at different rates and is controlled by the WAIFW (who acquires infection from whom) matrix β (6, 10, 13).

$$\beta = \begin{pmatrix} \beta_1 & \beta_1 & \beta_3 & \beta_4 \\ \beta_1 & \beta_2 & \beta_3 & \beta_4 \\ \beta_3 & \beta_3 & \beta_3 & \beta_4 \\ \beta_4 & \beta_2 & \beta_4 & \beta_4 \end{pmatrix}$$

To account for the school year, which plays a very important role (8, 9), the value of β_2 is decreased during school holidays. The WAIFW matrix (for both the RAS and PRAS models) is estimated by obtaining the best fit to the average biennial cycle from the England and Wales data. Full details are given in (12, 13).

15. R. M. Anderson and R. M. May, *IMA J. Math. Appl. Med. Biol.* **1**, 233 (1984); R. M. May and R. M. Anderson, *Math. Biosci.* **72**, 83 (1984); B. M. Bolker and B. T. Grenfell, *Philos. Trans. R. Soc. London Ser. B* **348**, 309 (1995).

16. M. J. Keeling and D. A. Rand, preprint (1996).
17. A. M. Lloyd and R. M. May, *J. Theor. Biol.* **179**, 1 (1996).
18. R. Engbert and F. R. Drepper, *Chaos Solitons Fractals* **4**, 1147 (1994); N. M. Ferguson, preprint (1996).
19. If we let P_E and P_I be the probability distribution functions of times in the two classes, then (ignoring mortality in the exposed and infectious classes) the standard SEIR model can be replaced by two time-delayed differential equations

$$\begin{aligned} dS/dt &= m(N - S) - \gamma \\ \frac{d\gamma}{dt} &= \frac{\gamma}{\beta} \frac{d\beta}{dt} + \frac{\gamma}{S} \frac{dS}{dt} + \beta S \int_0^\infty \gamma(t - \tau) A(\tau) d\tau \end{aligned} \tag{1}$$

where

$$A(\tau) = P_E(\tau) - \int_0^\tau P_I(T) P_E(\tau - T) dT$$

$\gamma = \beta SI$, m is the birth and death rate, and N is the population size. Although Eqs. 1 are useful from a mathematical perspective (23), for computational simplicity we further subdivide the E and I classes, so that individuals move into a new subclass after short time intervals. Deterministic simulations using these two methods give identical results.

20. R. E. Hope Simpson, *Lancet* **ii**, 549 (1952); N. J. T. Bailey, *Biometrika* **43**, 15 (1956).
21. N. J. T. Bailey, *The Mathematical Theory of Infec-*

tious Diseases (Griffin, London, 1975); F. C. Hoppensteadt, *J. Franklin Inst.* **297**, 325 (1974); Z. Grossman, *Theor. Popul. Biol.* **18**, 204 (1980).

22. M. Burnet and D. O. White, *Natural History of Infectious Diseases* (Cambridge Univ. Press, Cambridge, ed. 4, 1972).
23. For both the standard and revised modes, the average number of secondary infections caused by an infectious individual $[E(R_0)]$ are the same, as is the average infectious period $E(P_i)$. However when we consider the general form for the variance in R_0

$$\text{Var}(R_0) = E(R_0) + E(R_0)^2 \frac{\text{Var}(P_i)}{E(P_i)^2}$$

the standard RAS model with its exponential form for P_i (Fig. 3A) generates far greater variability in R_0 . This in turn leads to greater stochasticity and more extinctions, which can be highlighted by examining $P(0)$, the probability that an infectious individual will not produce any secondary cases (Fig. 3B)

$$P_{\text{RAS}}(0) = \frac{1}{1 + \beta S \bar{P}_i}, \quad P_{\text{PRAS}}(0) = e^{-\beta S E(P_i)}$$

24. D. Mollison, *Math Biosci.* **107**, 255 (1991).
25. ———, *Nature* **310**, 224 (1984).
26. We thank B. Bolker, S. Ellner, P. Harvey, and A. Kleczkowski for stimulating discussions. This research was supported by the Wellcome Trust and the Royal Society.

25 June 1996; accepted 15 October 1996

How Thiamine Diphosphate Is Activated in Enzymes

Dorothee Kern,*† Gunther Kern,‡ Holger Neef, Kai Tittmann, Margrit Killenberg-Jabs, Christer Wikner, Gunter Schneider, Gerhard Hübner

The controversial question of how thiamine diphosphate, the biologically active form of vitamin B₁, is activated in different enzymes has been addressed. Activation of the coenzyme was studied by measuring thermodynamics and kinetics of deprotonation at the carbon in the 2-position (C2) of thiamine diphosphate in the enzymes pyruvate decarboxylase and transketolase by use of nuclear magnetic resonance spectroscopy, proton/deuterium exchange, coenzyme analogs, and site-specific mutant enzymes. Interaction of a glutamate with the nitrogen in the 1'-position in the pyrimidine ring activated the 4'-amino group to act as an efficient proton acceptor for the C2 proton. The protein component accelerated the deprotonation of the C2 atom by several orders of magnitude, beyond the rate of the overall enzyme reaction. Therefore, the earlier proposed concerted mechanism or stabilization of a C2 carbanion can be excluded.

Coenzymes exert their catalytic activity after binding to a specific protein component. Therefore, it is crucial to understand how the reactivity of distinct groups of coenzymes is increased by interaction with the protein.

The coenzyme thiamine diphosphate (ThDP; Fig. 1), the biologically active derivative of vitamin B₁, is used by different enzymes that perform a wide range of catalytic functions. These include decarboxylation of 2-oxo acids and transketolation. Although the free coenzyme can assist some of these reactions, the protein environment potently accelerates the overall enzyme reaction by up to a factor of 10¹², as determined for pyru-

vate decarboxylase (PDC; E.C. 4.1.1.1) (1). The reactive C2 atom, located between the nitrogen and sulfur in the thiazolium ring, is the nucleophile that attacks the carbonyl carbon of the different substrates (2). For this reaction, the C2-ThDP atom must be activated by the enzyme environment. The deprotonation of C2 (Fig. 1) is the key reaction, because (i) this initial reaction is the only common step for all ThDP enzymes and (ii) the rate constant for this C-H dissociation is far too small in the free coenzyme compared with that of the entire enzyme reaction (3). The C2-ThDP activation in enzymes has been discussed for decades. In an early model, stabilization of ThDP C2-

carbanion in the enzyme-bound state was proposed (4). In contrast, a fast dissociation of the C2 proton in the enzyme-bound state could also explain the rate of the enzyme-mediated reaction (5). In a third model, a concerted pathway for the addition step of the substrate was described (6). Crystallographic studies of several ThDP-dependent enzymes (7–12) have revealed the molecular framework for enzymatic thiamin catalysis and, together with site-directed mutagenesis (13), have identified an invariant glutamate as a key feature in ThDP catalysis. However, the mechanism of cofactor activation could not be unambiguously elucidated.

To address this question, we analyzed the thermodynamics and kinetics of the deprotonation at C2 of ThDP in the enzymes PDC and transketolase (TK; E.C. 2.2.1.1) by nuclear magnetic resonance (NMR) spectroscopy. In addition, yeast PDC offers the possibility to study the mechanism of allosteric enzyme activation, because it is activated by its substrate (14, 15).

Apo-PDC tightly binds its coenzyme, ThDP, at pH values below 6.5, forming a 240-kD tetrameric enzyme which contains four ThDP/Mg²⁺ complexes (16). To study whether the protein shifts the equilibrium to detectable amounts of the C2 carbanion or whether the C2 remains protonated on the enzyme, we synthesized ¹³C-ThDP, recombined the labeled coenzyme with apo-PDC, and recorded the ¹³C-NMR spectra of the holoenzyme (17). The ¹³C-NMR spectrum of PDC with ¹³C2-labeled ThDP shows a distinct signal at 155 parts per million (ppm) that is missing in a spectrum of PDC containing the unlabeled coenzyme (Fig. 2). All other signals were identical in both spectra (data not shown). The signal at 155 ppm has the same chemical shift as the ¹³C2 signal of the free coenzyme, which is completely protonated in its C2 position. From these measurements, we conclude that the enzyme-bound ThDP does not exist as a discrete carbanion intermediate in detectable amounts in PDC, but rather prevails in its protonated form.

To study whether this equilibrium is shifted upon substrate activation, we used the nonconvertible substrate surrogate pyruvamide, which induces the active state

conformation by binding to the regulatory site (15). In the presence of pyruvamide, the signal at 155 ppm in the ¹³C2-ThDP containing PDC remains unchanged (Fig. 2C). Conclusively, the C2 is still protonated in the activated state.

Therefore, in the enzyme-catalyzed reaction, the addition of the carbonyl group of the substrate to C2 of ThDP requires either a fast dissociation of the C2 proton or a concerted mechanism. To discriminate between these two possibilities, the proton/deuterium (H/D) exchange kinetics of the proton bound to C2-ThDP in PDC were determined by ¹H-NMR (18). Figure 3 shows the time-dependent decay of the

C2-H signal (9.55 ppm) of ThDP resulting from the C2 H/D exchange of the coenzyme in the enzyme. The deprotonation in the enzyme-bound ThDP is accelerated by a factor of 10³ compared with that of free ThDP under the same conditions (Table 1). However, this rate constant is still one order of magnitude too small to allow the enzyme catalysis to proceed at the observed catalytic constant (*k*_{cat}) of 10 s⁻¹ at 4°C for each active site. Because the *k*_{cat} value represents the rate constant in the activated state, we also measured the kinetics of H/D exchange for C2-H of ThDP in the pyruvamide-activated PDC. The exchange was already complete within the shortest mix-

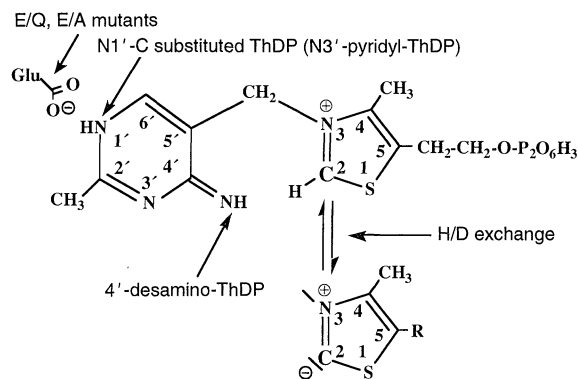


Fig. 1. The coenzyme ThDP is shown with the deprotonation step, common in all ThDP-dependent enzymes. Arrows indicate groups altered to elucidate the mechanism of cofactor activation; double arrows indicate the deprotonation step monitored directly by ¹³C and ¹H-NMR spectroscopy. E/Q and E/A refer to substitutions of the conserved glutamate to glutamine in PDC and alanine in TK.

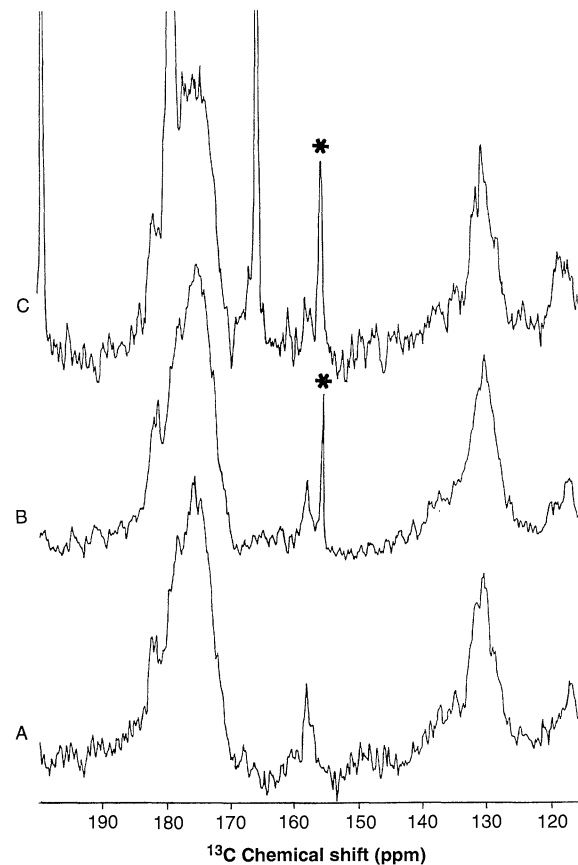


Fig. 2. Evidence for the protonation state of the C2 carbon of ThDP in nonactivated and activated PDC. Expansion of ¹H-decoupled ¹³C-NMR spectra of unlabeled (A) and ¹³C2-ThDP labeled yeast PDC in the absence (B) and in the presence (C) of 100 mM pyruvamide. The signal of ¹³C2-ThDP is marked with an asterisk and shows the same chemical shift as the protonated C2 carbon in free ThDP. The other signals originate from the natural abundance of ¹³C in the protein and relate to the carbonyl carbons (170 to 185 ppm), to the C^ε of arginine and C4 of tyrosine (155 to 157 ppm), and to some aromatic carbons (125 to 135 ppm). These signals were used to quantify the signal of C2-ThDP. The truncated signals in (C) originate from pyruvamide in its dehydrated and hydrated state.

D. Kern, G. Kern, H. Neef, K. Tittmann, M. Killenberg-Jabs, G. Hübner, Institut für Biochemie, Martin-Luther Universität Halle-Wittenberg, Kurt-Mothes-Straße 3, D-06120 Halle, Germany.

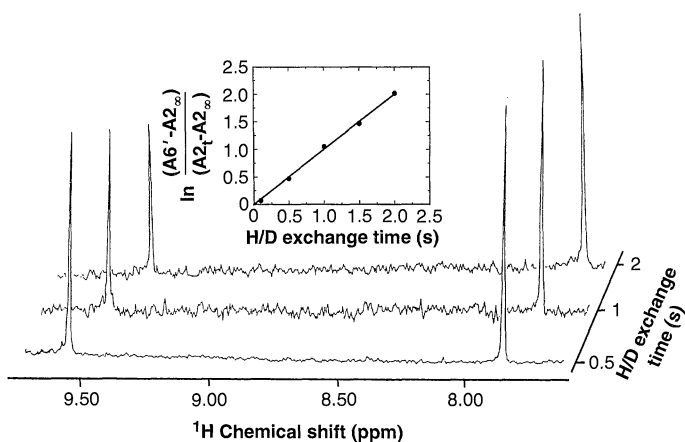
C. Wikner and G. Schneider, Karolinska Institutet, Department of Medical Biochemistry and Biophysics, Doktorsringen 4, S-17177 Stockholm, Sweden.

*To whom correspondence should be addressed.

†Present address: Department of Chemistry, University of California at Berkeley, Berkeley, CA 94720, USA.

‡Present address: Department of Molecular and Cellular Biology, University of California at Berkeley, Berkeley, CA 94720, USA.

Fig. 3. Kinetics of H/D exchange of ThDP C2-H in yeast PDC (18). The ^1H -NMR spectra are expansions showing the ThDP signals C2-H (9.55 ppm) and C6'H (7.85 ppm), the latter serving as a nonexchanging standard for quantification. To obtain the deprotonation rate, we fitted the decay in integral intensity of the C2-H signal to a pseudo-first order reaction (inset), where A_{2t} is the integral of the signal of the C2 proton at time t , $A_{2\infty}$ is that of the C2 proton after complete exchange, and $A_{6'}$ is that of the C6' proton.



ing time of the quench-flow apparatus (2 ms), resulting in a deprotonation rate which is at least three orders of magnitude higher than that of the nonactivated enzyme (Table 1). This shows that the C2-H dissociation—the crucial step in catalysis—is not rate limiting in activated yeast PDC, whereas it is rate limiting in the enzyme lacking allosteric activation. The activation process in yeast PDC is accomplished by an increase in the C2-H dissociation rate of the enzyme-bound coenzyme ThDP. This model was substantiated by measuring the H/D exchange of C2-H of ThDP in PDC from *Zymomonas mobilis*, which shows no substrate activation (19). As expected for this model, the deprotonation rate in *Z. mobilis* PDC is above its k_{cat} of 17 s^{-1} at 4°C for each active site (Table 1) and is not altered by pyruvamide.

To investigate whether the mechanism of ThDP activation is identical in other ThDP-dependent enzymes, H/D exchange experiments were performed with TK, which has a different substrate and reaction specificity. In fact, the common initial step in ThDP-mediated catalysis, the C2 deprotonation, is again not rate limiting ($k_{\text{cat}} = 8 \text{ s}^{-1}$), as observed for PDC (Table 1).

The crystal structures of the ThDP-dependent enzymes PDC (7, 12), transketolase (8, 9), and pyruvate oxidase (10, 11) show that the side chain of a glutamic acid is within a short distance of the N1' nitrogen of the pyrimidine ring, indicating formation of a hydrogen bond. Studies involving ThDP analogs in various ThDP-dependent enzymes point to a requirement for the N1' atom and 4'-NH₂ group of ThDP for catalytic activity (20, 21). On the basis of these findings, it has been proposed that the interaction between the glutamate and the N1' nitrogen enables the 4'-amino group to react in the proton translocation step (21, 22). In contrast, it has been argued that neither the glutamate-N1' interaction nor

the 4'-NH₂ group significantly contributes to the activation of ThDP, but rather that a base in the active site deprotonates the C2 (6).

To address this question, this glutamate and the closest base to C2 were mutated (23), and in addition, cofactor analogs lacking the 4'-amino group or the N1' were investigated.

The slow dissociation rate of C2-H in the glutamate mutants (Table 1) suggests that this glutamate is indeed involved in the proton abstraction mechanism of the enzyme-bound ThDP (24). In contrast, the mutation of the closest base to C2 in TK, His⁴⁸¹ → Ala (H481A), does not alter the rate of deprotonation (Table 1). Therefore, a mechanism in which His⁴⁸¹ is assumed to be the base for C2 proton abstraction (8) can be ruled out. X-ray structures of TK and its mutants show identical cofactor binding and no structural change of the protein component (13).

To unravel the function of the 4'-NH₂ group, TK was recombined with either the 4'-desamino form (25) or the N3'-pyridyl ThDP analog (26), whereas PDC could only be studied with 4'-desamino-ThDP because of the weak binding of N3'-pyridyl-ThDP. Both modifications of ThDP result in inactive enzymes and in a markedly decreased deprotonation rate of C2-H compared with the enzymes containing the natural coenzyme (Table 1). Structural changes were not detectable by x-ray crystallography (27). This establishes the essential function of both the 4'-amino group and the N1' in the deprotonation step.

We provide a clear and consistent model for the activation of ThDP in ThDP-dependent enzymes and for allosteric regulation of the yeast PDC. The directly determined C2 deprotonation rates show that a concerted mechanism, which was suggested on the basis of indirect measurements of C2-activation in ThDP (6), does not have to be

Table 1. Pseudo-first order rate constants for deprotonation of C2 in free and enzyme-bound coenzyme in 50 mM phosphate buffer at 4°C . PDC samples were measured at pH 6.0 and TK at pH 7.0. The experiments for determination of the rate constants are described in Fig. 3.

Sample	Rate constant (s ⁻¹)
Free ThDP (pH 6.0)	$9.5 \pm 0.4 \times 10^{-4}$
Free ThDP (pH 7.0)	$3.0 \pm 0.1 \times 10^{-3}$
Free 4'-desamino-ThDP (pH 6.0)	$1.2 \pm 0.1 \times 10^{-3}$
Free 4'-desamino-ThDP (pH 7.0)	$3.2 \pm 0.1 \times 10^{-3}$
Free N3'-pyridyl-ThDP (pH 7.0)	$1.6 \pm 0.1 \times 10^{-4}$
Yeast PDC (wild type)	$9.7 \pm 0.9 \times 10^{-1}$
Yeast PDC (wild type), pyruvamide-activated	$>6 \times 10^2$
Yeast PDC E51Q mutant	$7.6 \pm 0.6 \times 10^{-2}$
Yeast PDC E51Q mutant, pyruvamide-activated	1.7 ± 0.2
<i>Z. mobilis</i> PDC	$1.1 \pm 0.2 \times 10^2$
Yeast PDC recombined with 4'-desamino-ThDP	$3.4 \pm 0.1 \times 10^{-5}$
TK (wild type)	61 ± 2
TK E418A mutant	$3.7 \pm 0.1 \times 10^{-1}$
TK H481A mutant	61 ± 2
TK recombined with 4'-desamino-ThDP	$9.5 \pm 0.1 \times 10^{-5}$
TK recombined with N3'-pyridyl-ThDP	$1.6 \pm 0.2 \times 10^{-4}$

assumed to explain catalysis. Washabaugh and co-workers (6) measured much slower C2-H exchange rates for yeast PDC. However, the experimental conditions used were not appropriate for determination of activation of ThDP in the enzyme-bound state (28). In addition, our data from the ThDP analogs show that the N1' atom, as well as the 4'-NH₂ group, is essential for the activation of ThDP, which contradicts previously published assumptions (6).

The presented data support the following mechanism of the essential deprotonation step of the C2 atom in ThDP-dependent enzymes. In the enzyme-bound state, the C2 proton of ThDP is undissociated, as in free ThDP. However, the protein component dramatically accelerates the deprotonation, producing an intermediate C2 carbanion with a short lifetime. Fast deprotonation of C2 requires interaction of a glutamate with N1' in the pyrimidine ring, leading to an increased basicity of the 4'-amino group.

REFERENCES AND NOTES

1. F. J. Alvarez, J. Ermer, G. Hübner, A. Schellenberger, R. L. Schowen, *J. Am. Chem. Soc.* **113**, 8402 (1991).
2. R. Breslow, *ibid.* **80**, 3719 (1958); H. Holzer and K. Beaucamp, *Angew. Chem.* **71**, 776 (1959).
3. M. W. Washabaugh and W. P. Jencks, *Biochemistry* **27**, 5044 (1988).
4. J. Crosby and G. E. Lienhard, *J. Am. Chem. Soc.* **92**,

- 5707 (1970); D. S. Kemp and J. T. O'Brien, *ibid.*, p. 2554.
5. A. Schellenberger, *Angew. Chem. Int. Ed. Engl.* **6**, 1024 (1967); D. R. Petzold, *Stud. Biophys.* **54**, 159 (1976).
 6. E. J. Crane, J. A. Vaccaro, M. W. Washabaugh, *J. Am. Chem. Soc.* **115**, 8912 (1993); T. K. Harris and M. W. Washabaugh, *Biochemistry* **34**, 13994 (1995); *ibid.*, p. 14001.
 7. F. Dyda *et al.*, *Biochemistry* **32**, 6165 (1993).
 8. Y. Lindqvist, G. Schneider, U. Ermier, M. Sundström, *EMBO J.* **11**, 2373 (1992).
 9. M. Nikkola, Y. Lindqvist, G. Schneider, *J. Mol. Biol.* **238**, 387 (1994).
 10. Y. A. Muller and G. E. Schulz, *Science* **259**, 965 (1993).
 11. Y. A. Muller, G. Schuhmacher, R. Rudolph, G. E. Schulz, *J. Mol. Biol.* **237**, 315 (1994).
 12. P. Arjunan *et al.*, *ibid.* **256**, 590 (1996).
 13. C. Wikner *et al.*, *J. Biol. Chem.* **269**, 32144 (1994).
 14. A. Boiteux and B. Hess, *FEBS Lett.* **9**, 293 (1970).
 15. G. Hübner, R. Weidhase, A. Schellenberger, *Eur. J. Biochem.* **92**, 175 (1978).
 16. H. Zehender and J. Ullrich, *FEBS Lett.* **180**, 51 (1985).
 17. We synthesized ¹³C₂-ThDP according to (25), using 4-amino-5-aminomethyl-2-methylpyrimidine and ¹³C₅ (Isotec, 99 atom % ¹³C). We prepared ¹³C₂ ThDP-labeled PDC by recombination of 50 mg apo-PDC with 25 μmol of ¹³C₂-ThDP and 25 μmol of MgSO₄ in 1 ml of 0.1 M sodium phosphate buffer (pH 6.0). After separation of excess coenzyme by gel filtration with Sephacryl S 200 HR, the sample was concentrated to 40 mg of PDC per milliliter with a Millipore 10-kD membrane. The ¹H-decoupled ¹³C-NMR spectra were recorded in a 5-mm NMR tube on a Bruker AMX 500-MHz NMR spectrometer at 4°C (140,000 scans). After the NMR experiments, the PDC was precipitated by 3 M (NH₄)₂SO₄. No ¹³C₂-ThDP was detected in the supernatant, showing the absence of free ¹³C₂-ThDP in the samples used for spectra B and C (Fig. 2).
 18. The exchange reactions were initiated by dilution of a sample solution containing 30 mg of holoenzyme per milliliter or 1 mM coenzyme in 0.1 M sodium phosphate buffer (pH 6.0 for PDC and pH 7.0 for TK) with D₂O at a 1:1 ratio in a quenched-flow apparatus (Model RQF-3; Kin Tek Althouse, USA) for exchange times between 2 and 2000 ms or by manual mixing for longer mixing times. All pH values refer to the respective pH meter reading, which is a mixture between pH and pD. The exchange reactions were stopped by addition of DCl and trichloroacetic acid to final concentrations of 0.1 M and 5%, respectively (pH 0.9). In addition, this procedure rapidly and completely denatured and precipitated the protein and released the cofactor. All reactions were carried out at 4°C. After separation of the denatured protein by centrifugation, the ¹H-NMR spectra of the supernatant containing only the ThDP were recorded in a 5-mm NMR tube on a Bruker AMX 500-MHz NMR spectrometer.
 19. S. Bringer-Meyer, K. L. Schmitz, H. Sahn, *Arch. Microbiol.* **146**, 105 (1986).
 20. A. Schellenberger, *Chem. Ber.* **123**, 1489 (1970).
 21. R. Golbik *et al.*, *Bioorg. Chem.* **19**, 10 (1991).
 22. A. Schellenberger and G. Hübner, *Biochem. Educ.* **13**, 160 (1985); G. Schneider and Y. Lindqvist, *Bioorg. Chem.* **21**, 109 (1993); F. Jordan and Y. H. Mariam, *J. Am. Chem. Soc.* **100**, 2532 (1978); F. Jordan, G. Chen, S. Nishikawa, B. S. Wu, *Ann. N.Y. Acad. Sci.* **378**, 14 (1982); J. Koga, *Biochim. Biophys. Acta* **1249**, 1 (1995).
 23. The residual catalytic activity of the mutants, which bind ThDP as strongly as the wild-type enzymes, was 0.04% for Glu⁵¹ → Gln (E51Q) PDC (M. Killenberg-Jabs, S. König, I. Eberhardt, S. Hohmann, G. Hübner, *Biochemistry*, in press), 0.1% for Glu⁴¹⁸ → Ala (E418A) TK (13) and 4% for H481A TK (C. Wikner, U. Nilsson, L. Meshalkina, Y. Lindqvist, G. Schneider, in preparation).
 24. In addition, a comparatively small increase in the deprotonation rate by pyruvamide activation in the mutant PDC emphasizes that the signal transfer from the regulatory to the active center is probably mediated by E51. The structural events responsible for this step remain to be clarified.
 25. H. Neef, K.-D. Kohnert, A. Schellenberger, *J. Pract. Chem.* **315**, 701 (1973).
 26. A. Schellenberger, K. Wendler, P. Kreuzberg, G. Hübner, *Hoppe-Seyler's Z. Physiol. Chem.* **348**, 501 (1967).
 27. S. König, A. Schellenberger, H. Neef, G. Schneider, *J. Biol. Chem.* **269**, 10879 (1994).
 28. First, single-turnover conditions ([enzyme] > [substrate]), which were the basis for their calculations, are not valid because hydrolysis of the activator pyruvamide (100 mM) increases the initial pyruvate concentration (25 μM) above the enzyme concentration (50 μM). Second, the recombination of ThDP with apo-PDC was not complete within the used time, whereas our experiments were done with the intact holoenzyme after separation of excess free coenzyme. Third, our data explain why an isotope effect for C₂-hydrogen exchange could not be observed under the experimental conditions used. Within the recombination time of ThDP with PDC (20 s), the deuterium on C₂ of ThDP is completely replaced by a proton (Table 1).
 29. We thank D. Wemmer for critical reading of the manuscript. Supported by the Fond der Chemischen Industrie, the Deutsche Forschungsgemeinschaft, the Swedish Natural Science Research Council, and the National Board for Industrial and Technical Development.

20 August 1996; accepted 22 October 1996

Microtubule Architecture Specified by a β-Tubulin Isoform

Elizabeth C. Raff,* James D. Fackenthal,† Jeffrey A. Hutchens, Henry D. Hoyle, F. Rudolf Turner

In *Drosophila melanogaster*, a testis-specific β-tubulin (β₂) is required for spermatogenesis. A sequence motif was identified in carboxyl termini of axonemal β-tubulins in diverse taxa. As a test of whether orthologous β-tubulins from different species are functionally equivalent, the moth *Heliothis virescens* β₂ homolog was expressed in *Drosophila* testes. When coexpressed with β₂, the moth isoform imposed the 16-protofilament structure characteristic of that found in the moth on the corresponding subset of *Drosophila* microtubules, which normally contain only 13-protofilament microtubules. Thus, the architecture of the microtubule cytoskeleton can be directed by a component β-tubulin.

In eukaryotic cells, microtubules form diverse structures that are used for many different functions. Within each microtubule array, there are two levels of supramolecular organization: the architecture of each individual microtubule, determined by the number and arrangement of protofilaments, and the overall morphology of the microtubule array, for example, an axoneme or a spindle. Morphogenesis of each structure depends both on interactions between α- and β-tubulin heterodimers and on interactions between tubulins and other proteins. In vertebrate β-tubulins, isotype-defining variable regions (in particular the COOH-terminus), which have diverged among different isoforms in a gene family but are conserved in orthologs from different species, have been postulated to have an important role in conferring the functional specificity of each class of isoform (1). We previously demonstrated the validity of this hypothesis by showing that the unique COOH-

terminus of the *Drosophila melanogaster* testis-specific β₂-tubulin isoform is required for tissue-specific functions, including morphogenesis of the motile axoneme (2, 3). Spermatogenic-specific microtubule functions cannot be provided by β₃, another *Drosophila* β-tubulin isoform normally used during differentiation of a variety of somatic cells (3, 4).

Vertebrate β-tubulin orthologs in different species are conserved in structure and have similar expression patterns, suggesting that they perform similar functions (1). If this model is true for other groups of organisms of similar evolutionary relationship, then the β₂ ortholog from another insect should be better able to function in the *Drosophila* male germ cells than the paralogous β₃ isoform. A cDNA from the moth *Heliothis virescens* was reported that represents the gene for a testis-specific β-tubulin (Hvβt) whose expression pattern suggested it to be the moth β₂ ortholog (5). We sequenced the Hvβt clone and compared the predicted amino acid sequence with *Drosophila* β-tubulins. The COOH-termini of Hvβt and β₂ were more similar to each other than to the other *Drosophila* β-tubulins and exhibited the same relative similarities to the other *Drosophila* isoforms (Fig. 1A), substantiating that Hvβt is orthologous to β₂. How-

Department of Biology and Indiana Molecular Biology Institute, Indiana University, Bloomington, IN 47405, USA.

*To whom correspondence should be addressed. E-mail: eraff@bio.indiana.edu

†Present address: Department of Molecular Genetics and Cell Biology, University of Chicago, Chicago, IL 60637, USA.